PHYSICAL REVIEW E **74**, 040702(R) (2006)

Self-alignment of liquid crystals in three-dimensional photonic crystals

Stefano Gottardo,[1,*] Matteo Burresi,[1] Francesco Geobaldo,[2] Luca Pallavidino,[2] Fabrizio Giorgis,[3] and Diederik S. Wiersma[1]

[1]*European Laboratory for Nonlinear Spectroscopy and INFM-MATIS, via Nello Carrara 1, I-50019 Sesto Fiorentino (Florence), Italy*

[2]*Department of Material Science and Chemical Engineering, Polytechnical University of Torino, C. so Duca degli Abruzzi 24, I-10129 Turin, Italy*

[3]*Department of Physics, Polytechnical University of Torino, C. so Duca degli Abruzzi 24, I-10129 Turin, Italy*

(Received 13 March 2006; published 17 October 2006)

We report on the observation of self-alignment of nematic liquid crystals into colloidal photonic crystals, over distances much larger than the typical size of the voids between the spheres. We observe that the infiltrated structure possesses a unique optical axis that is determined by an intrinsic structural anisotropy of photonic crystal opals. We develop a simple model to describe this self-alignment based on the connectivity of the pores. The resulting structure constitutes a polarization dependent photonic crystal that can be controlled electrically.

DOI: 10.1103/PhysRevE.74.040702 PACS number(s): 61.30.Pq, 61.30.Hn, 42.70.Qs, 61.30.Gd

Liquid crystals in confined geometries exhibit a complex but fascinating physical behavior [1]. Such systems are obtained when liquid crystal is infiltrated in porous materials with, e.g., spherical, cylindrical, or randomly shaped voids. Of particular interest is the nematic phase in which the liquid crystal molecules tend to align along a common axis, called the nematic director, and otherwise are translationally disordered. Due to confinement in a porous material, the nematic-isotropic phase transition is, for instance, replaced by a continuous evolution of orientational order in the pores [2]. The alignment of a nematic director field inside a porous structure is extremely complex, due to the interaction between the liquid crystal molecules and the surface of the voids [3]. Anchoring of the liquid crystal molecules on the complex shaped surface deforms the director field and its final configuration will depend on the competition between surface anchoring and bulk elasticity [4].

When liquid crystals are incorporated in porous photonic structures one can control their optical properties. In that case one makes use of the optical birefringence of the nematic phase which can often be oriented by external electric or magnetic fields. Alternatively one can heat the system into the isotropic phase to change its refractive index. In the case of disordered photonic materials one can create this way diffusive systems of which the light diffusion constant can be controlled by external parameters such as temperature [5] or an electric field [6]. When liquid crystal is incorporated in ordered periodic structures, one can realize photonic crystals [7] of which the photonic bandgap can be influenced [8]. It is possible to tune a photonic bandgap by temperature [9] or electric field [10–12], which is potentially very interesting for applications in optical switching and controlled waveguiding. The nematic director field inside a photonic crystal is very complex and surface anchoring and other confinement effects usually impede electric field control over the nematic director [10,11]. However, Lavrentovich and Palffy-Muhoray turned this situation around by introducing the fascinating concept that liquid crystals in porous materials can self-align over large distances by the delicate interplay between bulk elastic and surface energies [13].

In this Rapid Communication we report on the observation of self-alignment of nematic liquid crystals in three-dimensional photonic crystals. We have studied photonic crystal opals infiltrated with liquid crystal in the nematic phase and observed optical birefringence due to self-alignment of the nematic director in a unique well-defined direction. This remarkable effect can be explained by the connectivity of the pores, according to Ref. [13], together with a small but intrinsic structural anisotropy of the photonic crystal. We can use this phenomenon to realize the first strongly polarization dependent photonic bandgap that can be controlled electrically.

Silica nanospheres were synthesized with the Stöber method [14]. We obtained controlled sphere radii R in the range of 60 nm to 320 nm with a standard deviation lower than 5%, verified by atomic and scanning electron microscopies. Silica opals were grown from these microsphere suspensions, using a dip-coating (DC) technique [15]. It consists of a self-assembly method which involves placing a nearly vertical substrate in the suspension of nanospheres (concentration 0.5–1 vol %). The opals were subsequently sintered at 850 °C for 3 hours. In addition to the opals grown by DC technique, a set of samples was realized by natural sedimentation (NS) for comparison.

We investigated the optical properties of such obtained direct opals by means of angular and wavelength resolved reflectivity measurements. A tungsten lamp was used as light source and the reflected light was monitored by a spectrometer and silicon detector (resolution 0.5 nm, spectral range 450–1100 nm). The principle of the experiment is shown in Fig. 1(a). The incident **k** vector lies in the x-y plane, and **p** and **s** indicate the polarization vectors for the incident light. The incident wavevector **k** could be rotated over a broad angular range: $\theta=5°-88°$. In addition, the sample could be rotated freely in the x-z plane over an angle $\varphi=0°-360°$, without moving the sample surface with respect to the illuminated spot. In Fig. 1(b) the reflectivity for a DC grown

*Email address: gottardo@lens.unifi.it; www.complexphotonics.org

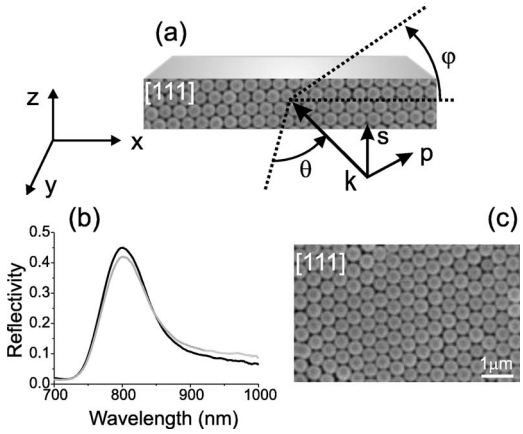

FIG. 1. (a) Geometry of the experiment. (b) Reflection spectra for **p** (black) and **s** (grey) polarization at $\theta=20°$ for a DC sample with $R=200$ nm. (c) SEM picture of the [111] plane for a DC sample ($R=200$ nm). The growing direction is along the z-axis.

sample is shown, for both **p** and **s** polarization at $\theta=20°$. As predicted by band diagram calculations [16] and observed for silica direct opals [17], the two polarization channels differ very weakly and only in the bandwidth of the stopband and not in their central wavelength. From Fig. 1(c), where a scanning electron microscope (SEM) picture is depicted, we can observe the [111] plane of a DC opal.

The silica opals were infiltrated with the liquid crystal E7 (Merck). Liquid crystal E7 is nematic in the temperature range from −10 °C to 60 °C, in which case it is birefringent with ordinary and extraordinary refractive index, respectively, $m_o=1.53$ and $m_e=1.75$ ($T=20$ °C) [18]. Upon infiltration, the stopband of the samples shifts to higher wavelengths due to the reduced refractive index contrast between the silica spheres and their environment. We observed, however, a completely different behavior for samples obtained by DC compared to NS growing technique. In addition to the redshift of the stopband, the DC samples became birefringent after infiltration. In Fig. 2, the results of several reflection measurements on the infiltrated DC samples are compiled. The central wavelength of the Bragg peak is plotted in function of the polarization angle α ($\alpha=0°$ corresponds to **p** polarization and $\alpha=90°$ to **s** polarization), for different values of the in-plane rotation angle of the sample φ. In Fig. 2(a) two cases are plotted: $\varphi=0°$ and $\varphi=90°$. We can clearly observe the birefringence of the sample: the central wavelength of the stopband strongly depends on polarization angle with a 180° periodicity. If we rotate the sample over $\varphi=90°$, we see that the polarization dependence is inverted, as expected. In Fig. 2(b) the cases $\varphi=30°$ and $\varphi=120°$ are reported, where we see that the polarization dependence is offset by the same angle. The optical axis of the infiltrated samples was found to lay on the x axis, orthogonal to the growing direction along z axis.

In order to verify that the observed birefringence of the photonic crystal is indeed due to the nematic liquid crystal infiltration and not due to artifacts, we heated the sample to $T=62$ °C, where the liquid crystal is in the isotropic phase. In Fig. 2(c) we observe that the birefringence disappears and no polarization dependence of the stopband can be observed in the isotropic phase.

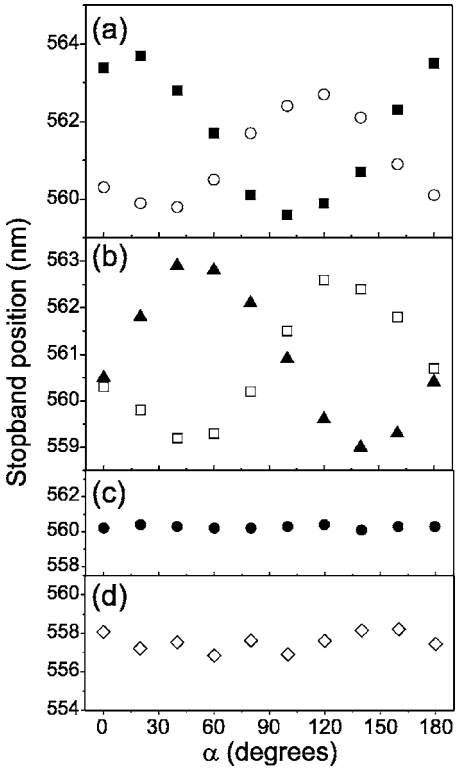

FIG. 2. Central wavelength of the photonic stopband for direct opal with $R=120$ nm infiltrated with liquid crystal vs polarization angle α ($\theta=20°$). (a) DC sample when $\varphi=0°$, 90° (black squares and open dots). (b) DC sample when $\varphi=30°$, 120° (black triangles and open squares). (c) DC sample heated into the isotropic phase at $T=62$ °C. (d) NS sample in the nematic phase.

To understand better the mechanism that leads to self-alignment of the nematic liquid crystal, we compared samples that were synthesized in different ways. In Fig. 2(d) the behavior of a sample with $R=120$ nm, prepared by natural sedimentation is shown, in which case the birefringence and hence the self-alignment of the liquid crystal is absent. Self-alignment of the liquid crystal was observed in all our samples prepared by dip-coating, but was never observed in samples prepared by natural sedimentation. This confirms that the DC process plays a fundamental role in the self-alignment of the liquid crystal, and that it is the structure of the sample that induces self-alignment of the liquid crystal. To examine the structural difference of the two growing technique for direct opals, SEM pictures of the samples were taken. We performed a two-dimensional Fourier transform (FT) of the images (30 μm × 30 μm) of the [111] plane of samples. For an ideal opal the FT from the [111] plane has to be a perfect hexagon. If the hexagon is elongated in one direction, it will mean that a spatial anisotropy is present on the [111] plane. The analysis revealed that the DC grown samples were, on average, 8% elongated in the direction orthogonal to the growth direction (x axis), whereas the NS samples were not. The DC grown samples are therefore not perfectly closed packed. This apparent artifact in the sample growth provides an enormous advantage for the liquid crystal infiltration since the connectivity of the pores increases. In addition, due to the anisotropy of the structure, the

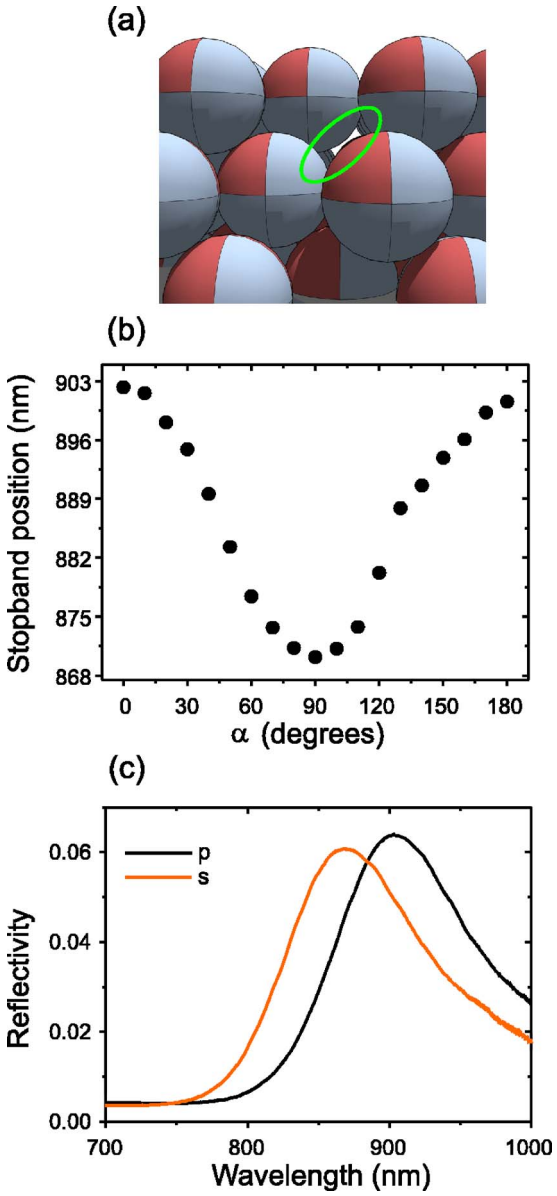

FIG. 3. (Color online). (a) Channel formed by stretching of 8% the [111] plane in one direction for a direct opal. stopband evolution for DC infiltrated direct opal ($R=200$ nm) in (b) and **p** and **s** spectra in panel (c), where $\theta=20°$.

stretched direction determines the overall preferred nematic director configuration.

A stretched direct opal along a direction in the [111] plane presents many open channels in different directions, and one of these is depicted in Fig. 3(a). The presence of these channels enhances drastically the connectivity between single voids for the DC samples. The optical birefringence can be even larger as observed for DC direct opals with larger spheres ($R=200$ nm), as shown in Fig. 3(b). We observe that the maximum wavelength difference between opposite polarizations **p** and **s** is in this case $\Delta\lambda \simeq 32$ nm. From Fig. 3(c), we observe that for **p** polarization, the reflection peak is redshifted, meaning that indeed the light experiences the extraordinary refractive index of the infiltrated direct opal.

To understand the behavior of a nematic liquid crystal inside a porous structure one has to take into account the surface anchoring strength W, the Frank elastic constant K, and the dielectric tensor ε of the liquid crystal. The actual voids in an opal have a very complex shape, being the residual space after packing of monodisperse spheres. One can take as the typical size L of these pores approximatively $L \cong 0.85\ R$ [10]. In nematic liquid crystals confined between boundary surfaces and in absence of an external field, the competition between the bulk elastic energy F_b and the surface energy F_s, determines the spatial distribution of the nematic director $\hat{n}$. Typically $F_b \cong \frac{1}{2}\int K(\nabla\cdot\hat{n})^2 dV$ and $F_s \cong \frac{1}{2}\int W \sin^2\gamma dS$, where γ is the angle between $\hat{n}$ and the preferred direction of the alignment at the surface. When we consider a network of interconnected pores, the ratio $F_s/F_b \sim WL^2/KL = L/\ell_e$, with $\ell_e = K/W$ the extrapolation length, determines which energy term dominates. If $F_s/F_b \gg 1$ ($L \gg \ell_e$) the surface effect dominates and the director $\hat{n}$ is spatially very inhomogeneous, meaning that $\langle\hat{n}\rangle = 0$. (The brackets denote averaging over a large volume of the sample.) When $F_s/F_b \ll 1$ ($L \ll \ell_e$), the equilibrium configuration is the one that minimizes the bulk elastic energy. Due to the connectivity of the pores, $\hat{n}$=const. is favored, which implies that the nematic director may be aligned and uniform over lengths L_d (typical domain size) much larger than ℓ_e [13]. The relation between L and L_d was calculated by Lavrentovich and Palffy-Muhoray for the case of randomly connected pores [13] with a certain degree of connectivity for the nematic subphase:

$$L_d = \frac{\ell_e^2}{L} + L. \tag{1}$$

If we use $K = 1.27 \times 10^{-11}$ N [19] and $W = 4 \times 10^{-6}$ J/m^2 (measured following Ref. [20]), we have for our samples $\ell_e \sim 3.2\ \mu$m, which is much larger than L. ($L \simeq 100$ nm for the $R=120$ nm samples and $L \simeq 170$ nm for the $R=200$ nm samples.) Hence the equilibrium configuration in our samples is indeed given by minimization of the bulk elastic energy. From Eq. (1) we find that self-alignment can be expected over domains as large as $L_d \sim 100\ \mu$m for the $R=200$ nm samples ($L_d \sim 60\ \mu$m for the $R=120$ nm samples). Since $L_d \gg R$, the self-alignment has a long-range nature.

Many measurements on infiltrated direct opals revealed, through the birefringence of the photonic stopband, that $\hat{n}$=const. over domains $L_d \geqslant 150\ \mu$m. From sample to sample it was possible to observe different behaviors, as depicted in Figs. 2(a) and 3(b), where the stopband moves, respectively, about 1% and 3%, basically because the amount of shift is determined by the orientation of the nematic director $\hat{n}$ with respect to the incoming wavevector **k**. The above-mentioned model is in agreement for DC sample, where the spatial anisotropy increases the connectivity of the nematic subphase [see Fig. 3(a)], while for NS samples it cannot be applied. The FT analysis for NS samples revealed a close-packed arrangement of the dielectric spheres, and hence the orientation of the director $\hat{n}$ follows the one proposed in Ref. [10], where no long-range order was observed.

The self-alignment of the liquid crystal along the [111] plane of the sample has an important advantage for possible

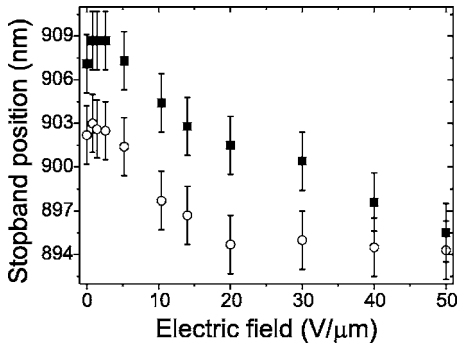

FIG. 4. Central wavelength of the stopband of the infiltrated DC opal with $R=200$ nm in function of the applied field E ($\theta=20°$). Black squares, **p** polarization and open circles, **s** polarization. The maximum shift is ≈ 13 nm. The error on the peak position was measured by observing fluctuations of the stopband for 30 sec.

electric field switching of the photonic bandgap. If one manages to apply a strong enough electric field orthogonal to the sample plane, it should be possible to change the nematic director alignment over 90°, such that an incoming extraordinary polarized light beam will experience the maximum possible change in refractive index contrast. To investigate the electric field dependence, we have prepared some samples between glass plates that were coated by a conducting coating of Indium doped Tin Oxide. This allowed to apply an electric field perpendicular to the [111] plane (along y axis) of the photonic crystal of up to about 50 V/μm.

In Fig. 4 the central wavelength of the stopband vs the electric field strength is reported for **p** and **s** polarization. We observe the following behavior. At very low field strength the position of the stopband remains unchanged. Above 5 V/μm, the central wavelength of the stopband starts to blueshift for both polarization channels, indicating that, globally, the nematic molecules start to align along the field direction. The blueshift is larger for the **p** polarization channel and at a field strength of about 50 V/μm the central wavelength in both polarization channels coincides. This means that at 50 V/μm the director alignment is perpendicular to the sample plane so that both polarization channels experience the ordinary refractive index of the liquid crystal. The overall blueshift observed in both polarization channels is very large ($\sim$13 nm for **p** polarization) and therefore perfectly suitable for electric field switching of the photonic crystal bandgap.

In conclusion, we observed self-alignment of nematic liquid crystal in periodic porous systems, consisting of photonic crystal opals, over distances larger than the typical size of the voids. The self-alignment could be attributed to a tiny structural anisotropy, inherent in the material synthesis, and is consistent with a model based on connected porous structures. The such obtained system constitutes a polarization dependent photonic crystal opal of which the polarization properties can be switched electrically. Interesting future investigations could involve, e.g., nuclear magnetic resonance experiments, to study the complex nematic director configuration in these fascinating photonic crystal materials.

We wish to thank Roberto Righini and Marcello Colocci for discussions, Willem Vos for discussions and careful reading of the manuscript, and Oleg Lavrentovich for stimulating discussions on confined nematics in porous systems. We acknowledge financial support from the EC network of excellence "Phoremost" (Grant No. IST-2-511616-NoE), and the MIUR Cofin project "Silicon Based Photonic Crystals."

[1] See, e.g., *Liquid Crystals in Complex Geometries*, edited by G. P. Crawford and S. Žumer (Taylor and Francis, London, 1996).
[2] G. S. Iannacchione *et al.*, Phys. Rev. Lett. **71**, 2595 (1993).
[3] A. Mertelj, L. Spindler, and M. Copic, Phys. Rev. E **56**, 549 (1997); L. Leclercq *et al.*, Liq. Cryst. **26**, 415 (1999).
[4] S. Zumer and J. W. Doane, Phys. Rev. A **34**, 3373 (1986); G. P. Crawford, D. W. Allender, and J. W. Doane, *ibid.* **45**, 8693 (1992); S. Basu and F. Aliev, Mol. Cryst. Liq. Cryst. **421**, 49 (2004).
[5] D. S. Wiersma *et al.*, Phys. Rev. B **64**, 144208 (2001).
[6] S. Gottardo *et al.*, Phys. Rev. Lett. **93**, 263901 (2004).
[7] J. D. Joannopoulos, R. D. Meade, and J. N. Winn, *Photonic Crystals: Molding the Flow of Light* (Princeton University, Princeton, NJ, 1995); K. Sakoda, *Optical Properties of Photonic Crystals* (Springer-Verlag, Berlin, 2001).
[8] K. Busch and S. John, Phys. Rev. Lett. **83**, 967 (1999).
[9] S. W. Leonard *et al.*, Phys. Rev. B **61**, R2389 (2000); G. Mertens *et al.*, Appl. Phys. Lett. **80**, 1885 (2002).
[10] D. Kang *et al.*, Phys. Rev. Lett. **86**, 4052 (2001).
[11] Y. Shimoda, M. Ozaki, and K. Yoshino, Appl. Phys. Lett. **79**, 3627 (2001); S. Gottardo, D. S. Wiersma, and W. L. Vos, Physica B **338**, 143 (2003).
[12] F. Du, Y.-Q. Lu, and S.-T. Wu, Appl. Phys. Lett. **85**, 2181 (2004); S. Kubo *et al.*, Chem. Mater. **17**, 2298 (2005); E. Graugnard *et al.*, Phys. Rev. B **72**, 233105 (2005).
[13] O. D. Lavrentovich and P. Palffy-Muhoray, Liq. Cryst. Today **5**, 5 (1995).
[14] W. Stöber, A. Fink, and E. Bohn, J. Colloid Interface Sci. **26**, 62 (1968).
[15] P. Jiang *et al.*, Chem. Mater. **11**, 2132 (1999).
[16] F. Lopez-Tejeira *et al.*, Phys. Rev. B **65**, 195110 (2002).
[17] J. F. Galisteo-Lopez *et al.*, Appl. Phys. Lett. **82**, 4068 (2003).
[18] D. Subacius, J. E. Stockley, and S. A. Serati, Proc. SPIE **3778**, 53 (1999).
[19] R. D. Polak *et al.*, Phys. Rev. E **49**, R978 (1994).
[20] V. S. U Fazio, F. Nannelli, and L. Komitov, Phys. Rev. E **63**, 061712 (2001).